**LETTER**

# Compatibility of pellet fuelling with ELM suppression by RMPs in the ASDEX Upgrade tokamak

View the article online for updates and enhancements.

# Letter

# Compatibility of pellet fuelling with ELM suppression by RMPs in the ASDEX Upgrade tokamak

**M. Valovič**[1] , **P.T. Lang**[2] , **A. Kirk**[1], **W. Suttrop**[2], **A. Bock**[2], **P.J. McCarthy**[3], **M. Faitsch**[2] , **B. Plöckl**[2], **the ASDEX Upgrade Team**[2] **and the EUROfusion MST1 Team**[a]

[1] CCFE, Culham Science Centre, Abingdon OX14 3DB, United Kingdom of Great Britain and Northern Ireland
[2] Max-Planck-Institut fűr Plasmaphysik, Boltzmannstrasse 2, D-85748 Garching, Germany
[3] Department of Physics, University College Cork, Cork, Ireland

E-mail: martin.valovic@ukaea.uk

CrossMark

## Abstract

It is demonstrated that tokamak plasma can be fuelled by pellets while simultaneously maintaining ELM suppression by external resonant magnetic perturbations (RMPs). Pellets are injected vertically from high field site and deposited at outer part of plasma cross section. Each pellet triggers a benign MHD event followed by a short lived ELM-free phase. The ELM suppression phase with pellet fuelling lasts 11 pellet cycles and is terminated by intentionally increasing the pellet rate to cause a transition to the ELMy phase.

Keywords: tokamak, pellet fuelling, ELM control

(Some figures may appear in colour only in the online journal)

## 1. Introduction

In tokamak fusion reactors such as ITER gas fuelling becomes inefficient and plasma density will be controlled by injection of hydrogen ice pellets [1, 2]. Simultaneously edge localised modes (ELMs) have to be avoided to protect exhaust system from large power excursions. One of the ELM control techniques is the application of external resonant magnetic perturbations (RMPs) [3–6] and such a system is planned on ITER [7]. Both pellet fuelling and RMPs act on the plasma periphery and therefore it is not surprising that these actuators are coupled as seen on DIII-D [3, 8–10], ASDEX Upgrade [11–14], MAST [15, 16] and EAST [17]. This coupling takes the form of two effects. Firstly, application of RMPs increases the peripheral particle transport (density pump out) which in turn has to be compensated by increased pellet fuelling. Secondly, fuelling pellets typically trigger ELMs and thus

counteract to ELM control. This letter describes an experiment where plasma is fuelled by pellets and simultaneously full ELM suppression is maintained. Our observation is the improovement of that described in DIII-D [8] where pellets were injected into the plasma with partial ELM suppression by RMPs. In this experiment, during the first two pellets the plasma stayed in ELM suppressed regime but later on plasma returned to partial ELM suppresssion. Another related experiment was performed in AUG [11]. In this experiment, however, the target plasma for pellet injection was different compared to that used in our present paper: the effect of magnetic perturbation was not resonant, the density pump out was not observed and the ELM mitigation occurred for densities higher than certain threshold. This is an opposite trend as observed for RMP ELM suppresssion at low collisionality. At low collisionality the transition to ELM suppression occurs below certain density. What is actual control parameter for transition to ELM suppression or mitigation is subject of active research and for details we refer to the references [18, 19].

1

## 2. Experimental setup

The experiment was performed on ASDEX Upgrade. In order to access the fully stationary ELM suppression phase the upper triangularity has to be elevated to about $\delta_u = 0.24$ [18, 20, 21]. In addition the plasma has a single null divertor, with radius of the geometric axis $R_{geo} = 1.58$ m, horizontal minor radius $a = 0.51$ m, plasma current $I_p = 0.94$ MA, toroidal field $B_T (R = 1.65 \text{ m}) = 1.78T$, safety factor $q_{95} = 3.7$. The plasma is heated by neutral beams with $P_{NBI} = 5.9$ MW. ELMs are controlled by RMP coils with toroidal periodicity $n = 2$ and for further details (see [18, 21]).

Pellet fuelling is provided by deuterium pellets injected vertically from the high field side with a velocity of 560 m s$^{-1}$ and a nominal size of $1.4 \times 1.4 \times 1.5$ mm. For this parameter set a total 30% of the pellet atoms are lost before the pellet arrives in the plasma reducing the effective pellet particle content to $N_{pel} = 1.2 \times 10^{20}$ atoms [22].

Key elements of this experiment are fresh boronisation and gradual reduction of gas fuelling. After application of RMPs the gas fuelling level is reduced to $\Phi_{gas} = 1 \times 10^{21}$ atoms s$^{-1}$ which allows the ELM suppressed phase to become established (see figure 1). A second gas reduction is introduced just before the pellet train when the gas is completely switched off. The pellet frequency is initially 23 Hz, and later increased to 47 Hz.

## 3. Pellet fuelling with suppressed ELMs

Figure 1 shows the effect of pellet fuelling on a plasma with simultaneous ELM suppression by RMPs. It is seen that during the 23 Hz pellet phase the peripheral plasma density transiently reaches the pre RMP value (figure 1(*a*)). In other words pellet fuelling broadly compensates for the density pump out and switching off the gas fuelling. At present there is no consensus which dimensionless parameter should be matched in order to demonstrate the relevance of this ELM/fuelling control method under ITER conditions. In this situation the selection of the pellet fuelling level that compensates for the density pump out and gas switch off seems to be a reasonable first choice.

Figure 1(*b*) shows the divertor tile current that is used as an indicator of ELMs, which manifest themselves as positive spikes. It is seen that during the first part of the pellet train from 2.8 s to 3.7 s there are infrequent irregular ELMs (see the positive spikes on the divertor current) indicating partial ELM suppression. This situation spontaneously changes during the second part of the pellet train from 4.1 s to 4.45 s where ELMs are completely suppressed. During this phase the density is slightly lower compared to the phase of partial ELM suppression. This is consistent with a notion of an empirical density threshold below which ELM suppression is observed (see the lower horizontal line in figure 1(*a*)). This is also in line with the plasma response to the increase of the pellet rate to 47 Hz which leads to a density increase and transition to ELMy H-mode. Figure 1(*e*) shows a reasonable separation between suppressed and ELMy data by the line of constant pressure. For

completeness figure 1(*e*) shows that the electron collisionality of plasmas with simultaneous ELM suppression and pellet fuelling is in the range of $\nu_e^* = 0.2 - 0.9$. Note that for high collissionality ELM suppression regime $\nu_e^* > 0.9$ [19]. Figure 1(*e*) also shows that on average the phase with ELM suppression and pellets have slightly (9%) higher pedestal top pressure compared to ELM suppression without pellets. This is due to increased density at constant temperature, figures 1(*a*) and (*c*). Such pedestal behaviour is reflected by global stored energy which does not change significantly (5%) after adding pellets at 2.7 s (for comparison the applicatioon of RMPs at 1.5 s reduces energy content by 20%). This behavior is similar to previous observations with ELM mitigation [14]. Finally note that in figure 1(*e*) there are about five ELMy points with pellets which are below the line of constant pressure. These are the data taken immediately after the pellet rate is increased to 47 Hz and as such represent the initial transient phase. All later ELMy data with pellets are above the line of constant pressure.

Figure 2 shows the details of plasma parameters during the quasi-stationary phase with full ELM suppression. The figure 2(*a*) shows the peripheral interferometer signal with each pellet causing a sharp density rise. Note that the pellet deposition is peripheral as seen from the electron density profile before and after the pellet in figure 2(*g*). The maximum of the density perturbation is located at $\rho_{pol} \sim 0.90$. This is similar to that expected in ITER [1, 23], however the ratio of pellet to plasma particles is about a factor of two larger than expected in ITER for fuelling pellets. To assess the interaction between pellet and RMP it is important to know the location of RMP affected area. If we assume that the affected area coincides with the location of $q = m/n$ resonance, then the relevant surface is $m/n = 7/2$ and it is localised at $\rho_{pol} = 0.96$ [21]. We therefore conclude that the RMP affected area is located more outside relative to the maximum of pellet deposition. This would imply that the direct interaction between pellet and RMP is mainly restricted to the time interval when pellet is inside the edge transport barrier.

The trace in figure 2(*c*) shows a magnetic pick up coils signal. It shows that each pellet triggers a short MHD spike. These events are not conventional ELMs. Firstly each such event causes a step like increase of the total plasma stored energy (figure 2(*f*)). These short transients are also visible on traces of the power to the divertor measured by the infrared camera showing the short dip after the pellet (see the divertor infrared camera signal in figure 2(*f*) red line). This behaviour is mirrored by the divertor tile current. All these observations are opposite to conventional ELMs which cause sudden energy loss and a corresponding spikes on a power to the divertor and on the divertor tile current.

To elaborate further on the character of MHD events, figure 3 compares two pellets, one in the phase of ELM suppression and one when ELM suppression is lost due to the increased pellet rate to 47 Hz (figure 1). It is seen that in both cases the MHD perturbations are synchronous with the pellet ablation light and similar in amplitude. The most striking difference is the divertor tile current $I_{div}$ which is a proxy to particle loss to the divertor. In the ELM suppressed case there
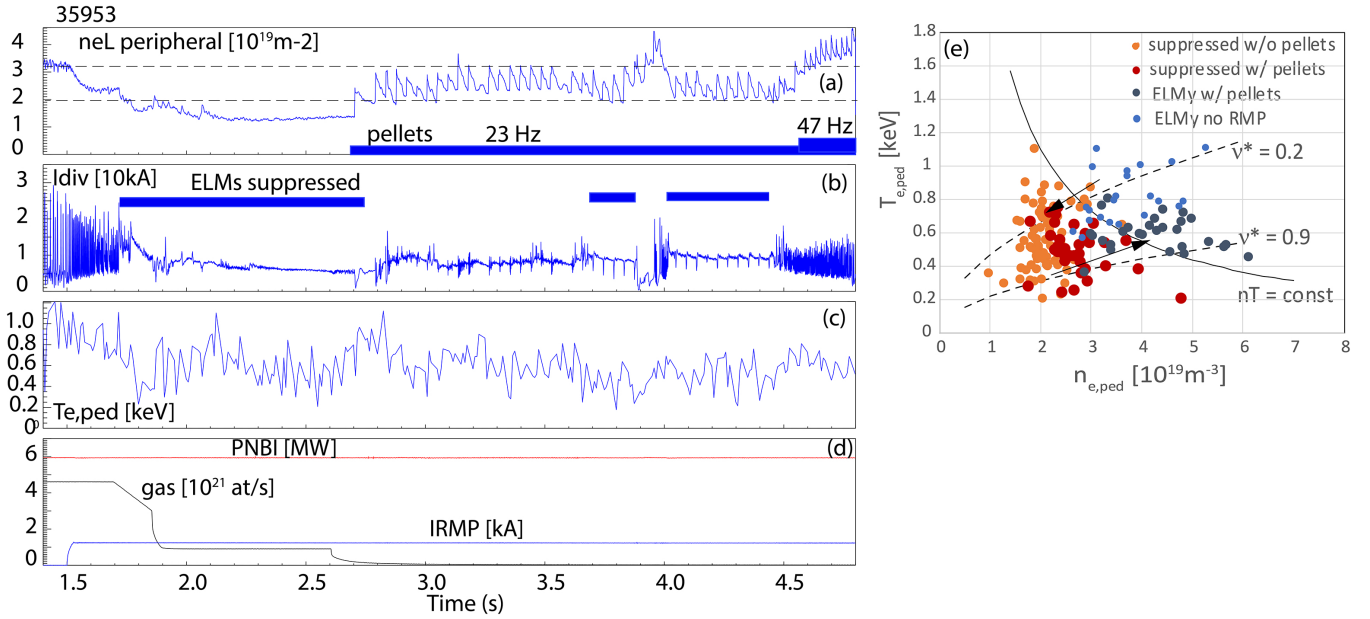
**Figure 1.** Pellet fuelling of plasma with ELM suppression by RMP. (*a*) Line integral density from the interferometer on peripheral chord $\rho_{pol} = \sqrt{\psi_N} > 0.8$, where $\psi_N$ is the normalised poloidal magnetic flux. (*b*) Divertor tile current—ELMs indicator, (*c*) electron temperature at pedestal top at $\rho_{pol} = 0.92$ by Thomson scattering (this radial position is dictated by the location of measurement points, see figure 2(*g*), (*d*) NBI power, gas puff rate and RMP current, (*e*) pedestal top electron temperature and density for different phases of the plasma on the left panels. Each data point represents one Thomson scattering measurement. Arrows indicate trajectory of evolution. The borderline phase 2.7–4.0 s is omitted for clarity in panel (*e*). ELMs before RMP are type-I with frequency of 90 Hz and 9.6% total plasma energy loss per ELM. The solid line represents constant electron pressure and the dashed line represents constant electron collisionality as used in [19]: $\nu_e^* = 6.921 \times 10^{-18} R_{geo} q_{95} n_e Z \ln \Lambda_e / \left( \epsilon^{3/2} T_e^2 \right)$ where $n_e$ is the electron density in m$^{-3}$, $Z = 1.5$, $\ln \Lambda_e \approx 15$, $\epsilon = a/R_{geo}$ and $T_e$ is the electron temperature in eV.
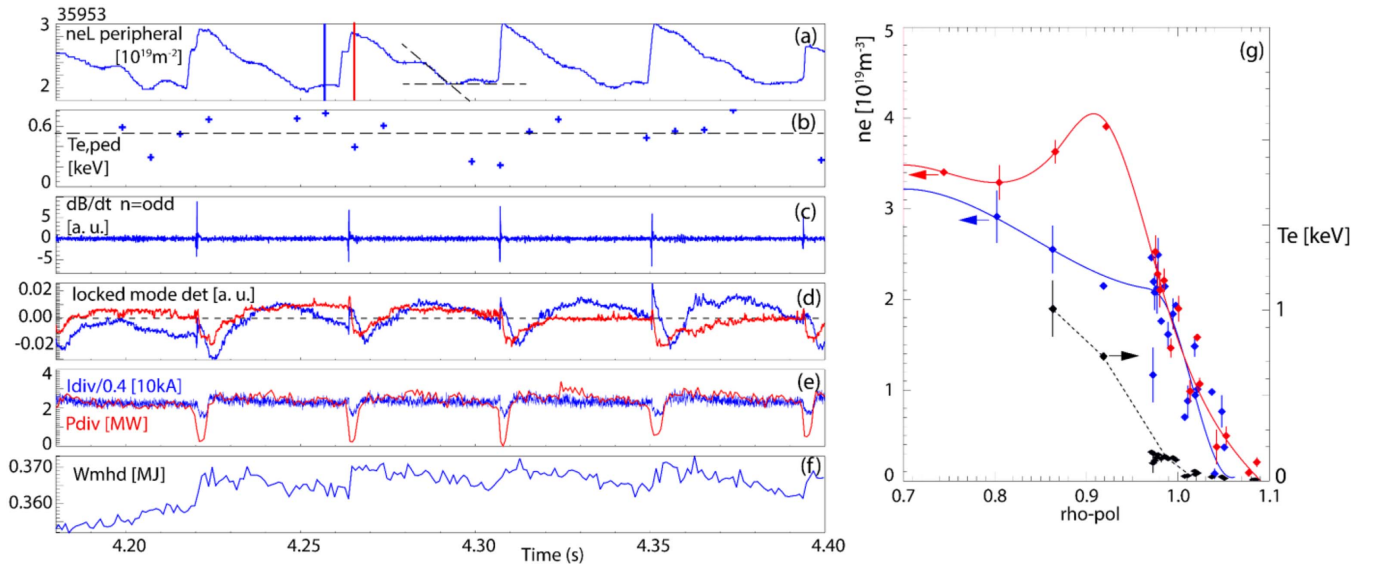


**Figure 2.** Quasi-stationary ELM suppressed phase (*a*) line integral density from the interferometer on peripheral chord (*b*) pedestal top electron temperature from Thomson scattering at $\rho_{pol} = 0.92$, (*c*) Mirnov coil signal, (*d*) locked mode detectors at different toroidal locations, (*e*) power to the divertor outer leg by the infrared camera (red) and divertor tile current (blue), (*f*) plasma energy content, (*g*) red and blue symbols: electron density profiles at times indicated by the vertical lines in panel (*a*); black symbols: electron temperature profile at time indicated by blue vertical line in panel (*a*).

is a very small increase of the divertor current by $\Delta I_{div} \sim$ 1.5 kA during the MHD perturbation before it drops at the end of the event. In the ELM case $I_{div}$ significantly increases during the MHD event by $\Delta I_{div} \sim 10$ kA, even displaying a correlation with oscillations on the magnetic signal. This trend

is the same on both inner and outer divertor legs. It is not clear whether these two type of events share the same MHD physics with the only difference that in the ELM suppressed case the MHD mode saturates (incomplete ELM). These events are benign and should be compatible with divertor operation.
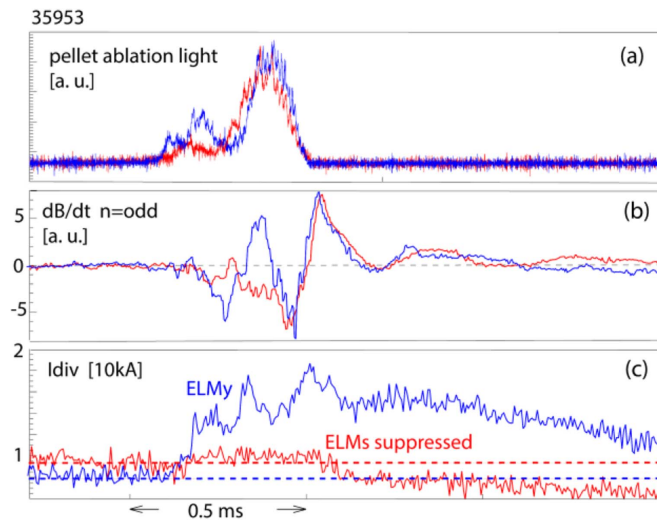
**Figure 3.** Comparison of pellet triggered magnetic perturbations in the ELMs suppressed phase (red, at $t_{pel} = 4.2630$ s) and the ELMy phase (blue, at $t_{pel} = 4.4795$ s). (*a*) Pellet ablation light, (*b*) Mirnov coil signals and (*c*) divertor current signals. Note that figure shows only initial part of the post pellet reduction of the divertor current.

The transient phases of reduced flux after pellets could be linked to a post pellet density profiles (figure 2(*g*)). It is seen that pellets create steep negative density gradient in the zone of $\rho_{pol} > 0.9$, similar to pellet triggered H-mode observed by several tokamaks [24–26]. This resembles formation of the edge transport barriers for heat and particle transport at the L–H transition but such phenomena were not reported during the H-mode. It has to be noted that in the context of ELM control, these phases are unfavourable because, if they last long enough, they open the possibility for spontaneous ELMs as seen in our previous experiment [14].

Finally it is interesting to note the behaviour of locked mode detector signals in figure 2(*d*). During pellet deposition there is a fast swing which is correlated with the spike on the magnetic pickup detector discussed above. After this fast event the locked mode signals slowly relaxes to the pre-pellet value. However this relaxation is not complete and a slow drift is evident during the shown time window indicating that the 3D equilibrium is evolving on a longer time scale (see the relative amplitude of two locked mode signals).

## 4. Conclusions

Thisletter reports on compatibility of pellet fuelling and ELM suppression by RMP, namely:

- fuelling pellets are shown to preserve ELM suppression by RMPs at low collisionality;
- individual pellets trigger benign MHD events; and
- the existence of ELM suppression with pellets is limited to below a certain pedestal density.

Future work should improve on stationarity of the phase with ELM suppression and pellet fuelling. This might be achieved by using both actuators, pellets and RMPs, in feedback mode. The future model of post pellet particle transport should explain how the pellet material is removed from the pellet deposition zone including the part with a positive density gradient.

## ORCID iDs

M. Valovič ⓘ https://orcid.org/0000-0002-0855-1056
P.T. Lang ⓘ https://orcid.org/0000-0003-1586-8518
M. Faitsch ⓘ https://orcid.org/0000-0002-9809-7490

## References

[1] Polevoi A.R. *et al* 2017 *Nucl. Fusion* **57** 022014
[2] Maruyama S. *et al* 2012 ITER fuelling and glow discharge cleaning system overview *Proc. 24th Int. Conf. on Fusion Energy* (San Diego, CA, (8-13 October 2012) (https://conferences.iaea.org/event/10/contributions/122/)
[3] Evans T.E. *et al* 2008 *Nucl. Fusion* **48** 024002
[4] Kirk A. *et al* 2012 *Phys. Rev. Lett.* **108** 255003
[5] Suttrop W. *et al* 2011 *Phys. Rev. Lett.* **106** 225004
[6] Liang Y. *et al* 2010 *Plasma Fusion Res.* **5** S2018
[7] Loarte A. *et al* 2014 *Nucl. Fusion* **54** 033007
[8] Baylor L.R. *et al* 2008 ELMs triggered from deuterium pellets injected into DIII-D and extrapolation to ITER *Proc. 35th EPS Conf. on Plasma Physics* (Hersonissos, Greece, 9-13 June 2008) P4.098 (http://epsppd.epfl.ch/Hersonissos/pdf/P4_098.pdf)
[9] Evans T.E. 2008 Implications of topological complexity and Hamiltonian chaos in the edge magnetic field of toroidal fusion plasmas *Chaos, Complexity and Transport: Theory and Applications*, ed C. Piere-Henri (Singapore: World Scientific Publishing Co. Pte. Ltd.) pp 147–76
[10] Evans T.E. *et al* 2013 *J. Nucl. Mater.* **438** S11
[11] Lang P.T. *et al* 2012 *Nucl. Fusion* **52** 023017
[12] Suttrop W. *et al* 2011 *Plasma Phys. Control. Fusion* **53** 124014
[13] Valovič M. *et al* 2016 *Nucl. Fusion* **56** 066009
[14] Valovič M. *et al* 2018 *Plasma Phys. Control. Fusion* **60** 085013
[15] Valovič M. *et al* 2013 *Plasma Phys. Control. Fusion* **55** 025009
[16] Valovič M. *et al* 2015 *Nucl. Fusion* **55** 013011
[17] Hou J. *et al* 2019 *Nucl. Fusion* **59** 096039
[18] Suttrop W. *et al* 2017 *Plasma Phys. Control. Fusion* **59** 014049
[19] Kirk A. *et al* 2015 *Nucl. Fusion* **55** 043011
[20] Evans T.E. *et al* 2004 *Phys. Rev. Lett.* **92** 235003
[21] Suttrop W. *et al* 2018 *Nucl. Fusion* **58** 096031
[22] Lang P.T. *et al* 2003 *Rev. Sci. Instrum.* **74** 3974
[23] Garzotti L. *et al* 2019 *Nucl. Fusion* **59** 026006
[24] Askinazi L.G. *et al* 1993 *Phys. Fluids* B **5** 2420
[25] Gohil P. *et al* 2001 *Phys. Rev. Lett.* **86** 644
[26] Valovič M.*et al*2012*Nucl. Fusion***52**114022